Journal of Sound and Vibration (2002) **255**(5), 849–866
doi:10.1006/jsvi.2001.4189, available online at http://www.idealibrary.com on IDEAL®

FINITE ELEMENT AND BOUNDARY ELEMENT MODELLING FOR THE ACOUSTIC WAVE TRANSMISSION IN MEAN FLOW MEDIUM

T. Tsuji†, T. Tsuchiya and Y. Kagawa

Department of Electronics and Information Systems, Akita Prefectural University, Honjo, Akita 015-0055, *Japan. E-mail: y.kagawa@akita-pu.ac.jp*

(*Received* 10 *May* 2001, *and in final form* 20 *November* 2001)

The frequency characteristics of the acoustic wave transmission in a medium with mean flow are considered. One approach is to solve the Helmholtz equation with mean flow medium in original co-ordinates, which is directly discretized for the one-dimensional and the axisymmetric FEM. Another approach is to transform the equation into the standard Helmholtz equation, which is discretized for the axisymmetric FEM and the three-dimensional BEM. The numerical models are examined first for a straight circular duct. The solutions by the numerical approaches are compared with the analytical solution. The examination is then extended to the case when the mean flow is locally present in the muffler with expansion chamber. To model the spatial mean flow in the BEM model, the partitioned domain approach is also developed. No shear effect between the two regions are included.
© 2002 Elsevier Science Ltd. All rights reserved.

1. INTRODUCTION

A duct with variable cross-section is the acoustic wave transmission system which has an important field of applications. Its numerical solution has been arrived at by many investigators [1–5]. Its acoustic wave transmission characteristic is however affected by the presence of the medium motion. First of all, the propagation velocity may decrease for the waves against the stream, while it may increase for the waves along the stream. This is the case when the waves transmit in the exhaust muffler of the automobiles and also in the vocal tract. The wave equation and Helmholtz equation under such a condition have already been presented in the book by Munjal [6] in which analytical solution in one dimension is also given. Some experimental investigations were made in the dissertation by Chattajee [7]. For two and three-dimensional counterparts, the numerical approach must be devised. The boundary element approach was presented by Zhenlin *et al.* [8], in which the equation is transformed to the standard Helmholtz equation by means of the co-ordinate transformation. All the treatments are made for the steady state waves in frequency domain. For the time-domain wave propagation in mean flow, the present authors proposed the discrete Huygens approach [9].

In the present paper, the analytical solution in one dimension is extended to the case of the general impedance termination. The numerical solution by the finite element approach is compared with the analytical solution. The finite element modelling is then applied to the axisymmetric case in which the formulation is made both for the original and transformed co-ordinates. The boundary element approach presented by Zhenlin *et al.* is extended to the

† Present affiliation: Kyosera-Mita Co. Ltd., Osaka, Japan.

0022-460X/02/$35.00 © 2002 Elsevier Science Ltd. All rights reserved.

case of the spatial mean flow, which is treated by the partition domain approach. Numerical examples for the duct with an expansion chamber are then demonstrated.

2. GOVERNING EQUATIONS

2.1. WAVE EQUATION IN THE MEDIUM IN MEAN FLOW

Here, we consider the sound wave propagation in a medium with uniform and steady state mean flow. The medium is also assumed to be homogeneous and non-dissipative. The fluid dynamics is expressed in terms of three basic dynamics equations [6]. The first is the equation of continuity,

$$\frac{\partial \rho}{\partial t} + \nabla \cdot \{(\rho_0 + \rho)(\mathbf{V}_0 + \mathbf{u})\} = 0, \tag{1}$$

where ρ is the excess density resulting from the acoustic disturbance, ρ_0 is the ambient density, $\mathbf{u}$ is the particle velocity, $\mathbf{V}_0$ is the mean flow and t refers to time. The second is the equation of motion,

$$(\rho_0 + \rho)\left\{\frac{\partial \mathbf{u}}{\partial t} + (\mathbf{V}_0 + \mathbf{u}) \cdot \nabla(\mathbf{V}_0 + \mathbf{u})\right\} = -\nabla p, \tag{2}$$

where p is the sound pressure. The last is the equation of the state, when the pressure is expanded about the ambient pressure,

$$P = P_0 + A\left(\frac{\rho - \rho_0}{\rho_0}\right) + \frac{B}{2}\left(\frac{\rho - \rho_0}{\rho_0}\right)^2 + \cdots, \tag{3}$$

where $P(= P_0 + p)$ is the pressure, P_0 is the ambient pressure, $A = \rho_0 c_0^2$, $B = \rho_0^2\, \partial^2 P/\partial \rho^2$ when the entropy is constant, c_0 is the sound speed at small amplitude. These equations can be linearized by discarding the second order terms to form

$$\frac{\partial \rho}{\partial t} + \mathbf{V}_0 \cdot \nabla \rho + \rho_0 \nabla \cdot \mathbf{u} = 0, \quad \rho_0\left(\frac{\partial \mathbf{u}}{\partial t} + \mathbf{V}_0 \nabla \cdot \mathbf{u}\right) = -\nabla p, \quad p = c_0^2 \rho. \tag{4–6}$$

From these equations, the linear wave equation in a medium in mean flow can be derived as

$$\nabla^2 p - \frac{1}{c_0^2}\frac{\partial^2 p}{\partial t^2} - \frac{2}{c_0^2}\frac{\partial}{\partial t}(\mathbf{V}_0 \cdot \nabla p) - \frac{1}{c_0^2}(\mathbf{V}_0 \cdot \nabla)(\mathbf{V}_0 \cdot \nabla p) = 0 \tag{7}$$

or

$$\nabla^2 p - \frac{1}{c_0^2}\frac{\partial^2 p}{\partial t^2} - \frac{2}{c_0}\frac{\partial}{\partial t}(\mathbf{M} \cdot \nabla p) - (\mathbf{M} \cdot \nabla)(\mathbf{M} \cdot \nabla p) = 0, \tag{8}$$

where $\mathbf{M} = \mathbf{V}_0/c_0$ is Mach number of the mean flow.

The particle velocity $\mathbf{u}$ and the sound pressure p can be expressed in terms of the velocity potential ϕ, as

$$\mathbf{u} = -\nabla \phi, \qquad p = \rho_0\left(\frac{\partial \phi}{\partial t} + \mathbf{V}_0 \cdot \nabla \phi\right). \tag{9, 10}$$

Wave equation (8) can be rewritten for the velocity potential as

$$\nabla^2\phi - \frac{1}{c_0^2}\frac{\partial^2\phi}{\partial t^2} - \frac{2}{c_0}\frac{\partial}{\partial t}(\mathbf{M}\cdot\nabla\phi) - (\mathbf{M}\cdot\nabla)(\mathbf{M}\cdot\nabla\phi) = 0. \tag{11}$$

In the steady state harmonic motion ($\phi = \Phi e^{j\omega t}$, where Φ is the amplitude of the potential, $\omega = 2\pi f$ is the angular frequency and f is the frequency), wave equation (11) can be expressed as

$$\nabla^2\Phi + k^2\Phi - j2k(\mathbf{M}\cdot\nabla\Phi) - (\mathbf{M}\cdot\nabla)(\mathbf{M}\cdot\nabla\Phi) = 0, \tag{12}$$

where $k = \omega/c_0$ is the wave number. In the following analysis, the medium is assumed to be moving in the z direction, so that the governing equation is given by

$$\nabla^2\Phi + k^2\Phi - j2kM_z\frac{\partial\Phi}{\partial z} - M_z^2\frac{\partial^2\Phi}{\partial z^2} = 0, \tag{13}$$

where M_z is the mean flow Mach number in the z direction.

2.2. HELMHOLTZ EQUATION IN TRANSFORMED CO-ORDINATES

With the following co-ordinate and variable transformations,

$$\tilde{x} = x,\ \tilde{y} = y, \quad \tilde{z} = \frac{z}{\sqrt{1 - M_z^2}}, \qquad \tilde{k} = \frac{k}{\sqrt{1 - M_z^2}}, \tag{14}$$

$$\tilde{\Phi} = \Phi e^{-jkM_z z}, \tag{15}$$

equation (13) leads to the standard Helmholtz equation with respect to $\tilde{\Phi}$ as

$$\tilde{\nabla}^2\tilde{\Phi} + \tilde{k}^2\tilde{\Phi} = 0, \tag{16}$$

where $\tilde{\nabla}^2$ is the Laplacian operator in the transformed co-ordinates. This expression is numerically solved by Zhenlin *et al.* [8] with the help of the boundary element approach. The equation is thus simplified at the expense of the complicated boundary conditions. This means that the numerical analysis program such as the finite elements or boundary elements developed for the standard Helmholtz equation can be used without modification, but with the potential and the boundary conditions re-defined.

3. ONE-DIMENSIONAL FIELD

3.1. MODEL

Now, we consider the wave transmission in a duct as shown in Figure 1. The duct is driven by uniform velocity U_0 at one end ($z = 0$) and it is acoustically terminated by the surface acoustic impedance Z_T at another end ($z = l$). The boundary conditions for this case

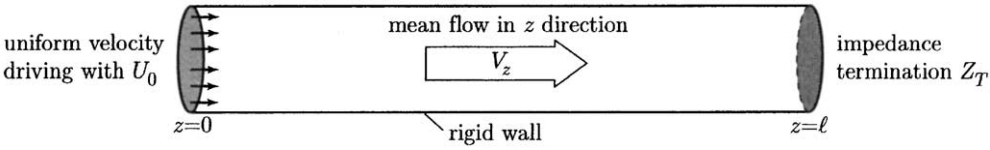

Figure 1. A duct in mean flow.

correspond to

$$\frac{\partial \Phi}{\partial n} = -\frac{\partial \Phi}{\partial z} = U_0 \quad (z = 0),$$

$$\frac{\partial \Phi}{\partial n} = \frac{\partial \Phi}{\partial z} = -\mathrm{j}k\frac{1}{\beta_T + M_z}\Phi \quad (z = l),$$

$$\frac{\partial \Phi}{\partial n} = 0 \quad \text{(wall boundary)}, \tag{17}$$

where $\partial/\partial n$ is the normal derivative to the boundary and $\beta_T = Z_T/\rho_0 c_0$ is the termination impedance normalized with respect to the characteristic impedance of the medium.

3.2. ANALYTICAL SOLUTION

For the one-dimensional field in which the wave propagates toward the z direction, equation (13) is reduced to

$$(1 - M_z^2)\frac{\partial^2 \Phi}{\partial z^2} + k^2\Phi - \mathrm{j}2kM_z\frac{\partial \Phi}{\partial z} = 0. \tag{18}$$

The general solution is of the form

$$\Phi(z) = C_1 \mathrm{e}^{-\mathrm{j}kz/(1+M_z)} + C_2 \mathrm{e}^{\mathrm{j}kz/(1-M_z)}, \tag{19}$$

where C_1 and C_2 are the coefficients to be determined. The first term on the right-hand side expresses the sound propagating to the z direction and the second term the one propagating to the reverse $-z$ direction. From equations (9) and (10), the particle velocity and the sound pressure are, respectively, obtained as

$$U(z) = \mathrm{j}k\left(\frac{C_1}{1+M_z}\mathrm{e}^{-\mathrm{j}kz/(1+M_z)} - \frac{C_2}{1-M_z}\mathrm{e}^{\mathrm{j}kz/(1-M_z)}\right), \tag{20}$$

$$P(z) = \mathrm{j}\omega\rho_0\left(\frac{C_1}{1+M_z}\mathrm{e}^{-\mathrm{j}kz/(1+M_z)} + \frac{C_2}{1-M_z}\mathrm{e}^{\mathrm{j}kz/(1-M_z)}\right). \tag{21}$$

The coefficients C_1 and C_2 are determined by the boundary condition. The analytical solution for the sound pressure under boundary condition (17) is

$$P(z) = \frac{-(\rho_0 c_0 - Z_T)\mathrm{e}^{-\mathrm{j}k(l-(1+M_z)z)/(1-M_z^2)} + (\rho_0 c_0 + Z_T)\mathrm{e}^{\mathrm{j}k(l-(1-M_z)z)/(1-M_z^2)}}{(\rho_0 c_0 - Z_T)\mathrm{e}^{-\mathrm{j}kl/(1-M_z^2)} + (\rho_0 c_0 + Z_T)\mathrm{e}^{\mathrm{j}kl/(1-M_z^2)}} \rho_0 c_0 U_0. \quad (22)$$

3.3. FINITE ELEMENT FORMULATION

We solve equation (18) by the finite element method. The equation is discretized in space by a Galerkin's procedure. The weak formation is

$$\int \left\{(1-M_z^2)\frac{\partial\varphi}{\partial z}\frac{\partial\Phi}{\partial z} - k^2\varphi\Phi + \mathrm{j}2kM_z\varphi\frac{\partial\Phi}{\partial z}\right\}\mathrm{d}z = (1-M_z^2)\varphi\frac{\partial\Phi}{\partial n}\bigg|_\Gamma, \quad (23)$$

where φ is a weighting function and Γ denotes the boundary. In the Galerkin's method, the weighting function is usually chosen to be the test function ($\varphi = \Phi$). The right-hand side of equation (23) corresponds to the boundary condition (17). The one-dimensional region to be analyzed is divided into line elements. The velocity potential in an element is interpolated by the nodal velocity potentials so that

$$\Phi = \{N\}^{\mathrm{T}}\{\Phi\}_e \quad (24)$$

where $\{\Phi\}_e$ is the nodal velocity potential vector, $\{N\}$ is the interpolation function vector. The superscript T denotes the transpose of matrix or vector. The velocity potential is here assumed to be linearly interpolated within a line element.

Substituting equation (24) into equation (23), one has the discretized equation for an element

$$\left\{(1-M_z^2)[M]_e - k^2[K]_e + \mathrm{j}k\left(2M_z[V]_e + \frac{1-M_z^2}{\beta_T + M_z}[J]_e\right)\right\}\{\Phi\}_e = U_0(1-M_z^2)\{W\}_e, \quad (25)$$

where $[M]_e$, $[K]_e$, $[V]_e$ and $[J]_e$ are inertance, elastance matrices, the matrix associated with mean flow and the wall dissipation and $\{W\}_e$ is the distribution vector. It should be noticed that the matrix $[V]_e$ associated with the mean flow is non-symmetric. The presence of the flow may act as a damping.

4. AXISYMMETRIC FIELD

4.1. FINITE ELEMENTS IN ORIGINAL CO-ORDINATES

For the axisymmetric field, equation (13) can be expressed as

$$\frac{\partial}{\partial r}\left(r\frac{\partial\Phi}{\partial r}\right) + (1-M_z^2)\frac{\partial}{\partial z}\left(r\frac{\partial\Phi}{\partial z}\right) + rk^2\Phi - \mathrm{j}2rkM_z\frac{\partial\Phi}{\partial z} = 0. \quad (26)$$

Galerkin procedure for the axisymmetric field leads to another weak form as

$$2\pi\iint\left\{r\frac{\partial\varphi}{\partial r}\frac{\partial\Phi}{\partial r} + r(1-M_z^2)\frac{\partial\varphi}{\partial z}\frac{\partial\Phi}{\partial z} - rk^2\,\varphi\,\Phi + \mathrm{j}2rkM_z\varphi\frac{\partial\Phi}{\partial z}\right\}\mathrm{d}r\,\mathrm{d}z$$
$$= 2\pi\int r(1-M_z^2)\varphi\frac{\partial\Phi}{\partial n}\mathrm{d}\Gamma. \quad (27)$$

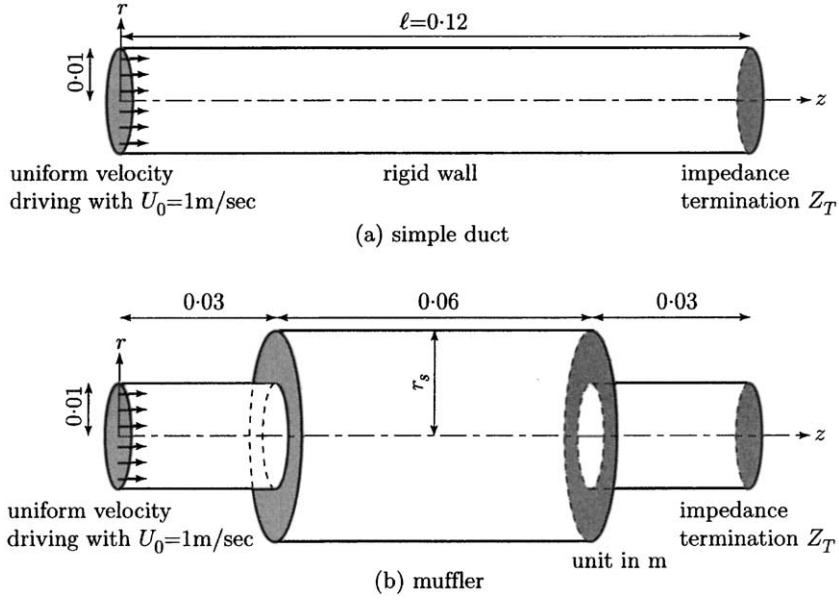

Figure 2. Simple duct and muffler.

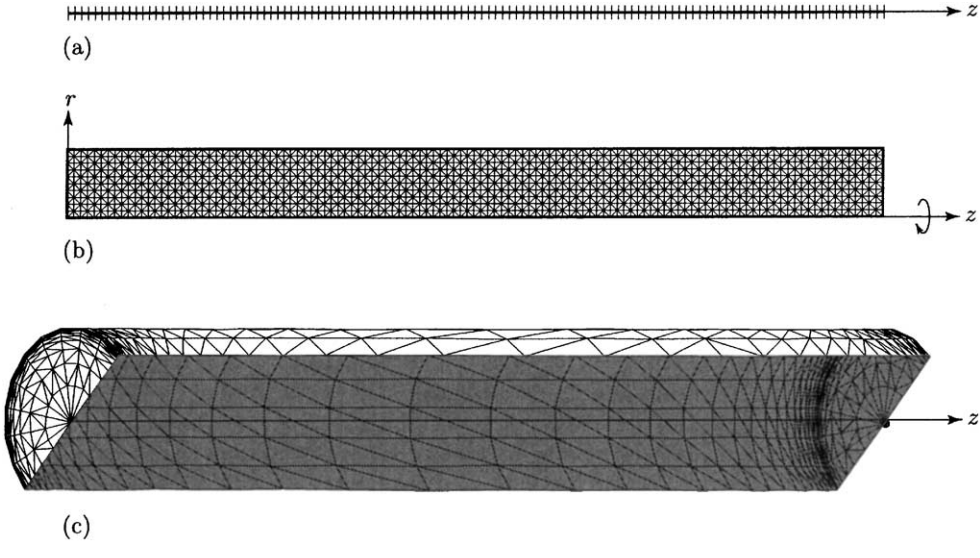

Figure 3. Numerical models for a simple duct: (a) one-dimensional FEM model; (b) axisymmetric FEM model; (c) three-dimensional BEM model.

In the axisymmetric case, the cross-sectional area to be analyzed is divided into triangular ring elements. The test function has the same form as equation (24), but with three nodes. The final discretized expression is again the same as the one-dimensional case (equation (25)).

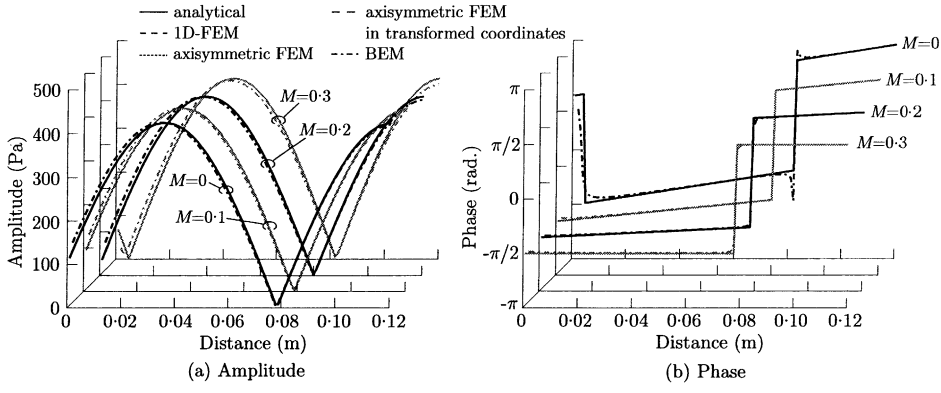

Figure 4. Sound pressure distributions along the central z-axis in a simple duct for various Mach numbers M ($f = 2$ kHz and the duct is terminated at one end by the rigid wall $Z_T = \infty$).

4.2. FORMULATION IN TRANSFORMED CO-ORDINATES

4.2.1. *Finite element formulation*

In the transformed co-ordinates, the Helmholtz equation is obtained from equation (16) for the cylindrical co-ordinates and the expression is

$$\frac{\partial}{\partial \tilde{r}}\left(\tilde{r}\frac{\partial \tilde{\Phi}}{\partial \tilde{r}}\right) + \frac{\partial}{\partial \tilde{z}}\left(\tilde{r}\frac{\partial \tilde{\Phi}}{\partial \tilde{z}}\right) + \tilde{r}\tilde{k}^2\tilde{\Phi} = 0. \tag{28}$$

The normal derivative to the boundary or flux can be expressed as

$$\frac{\partial \tilde{\Phi}}{\partial \tilde{n}} = \left(\frac{\partial \Phi}{\partial n}\frac{\partial n}{\partial \tilde{n}} - \mathrm{j}\tilde{k}M_z\Phi\frac{\partial \tilde{z}}{\partial \tilde{n}}\right)\mathrm{e}^{-\mathrm{j}\tilde{k}M_z\tilde{z}}. \tag{29}$$

So the boundary conditions corresponding to equation (17) are

$$\frac{\partial \tilde{\Phi}}{\partial \tilde{n}} = U_0\sqrt{1 - M_z^2} - j\tilde{k}M_z\tilde{\Phi} \quad (z = 0),$$

$$\frac{\partial \tilde{\Phi}}{\partial \tilde{n}} = -\mathrm{j}\tilde{k}\frac{1 + \beta_T M_z}{\beta_T + M_z}\tilde{\Phi} \quad (z = l),$$

$$\frac{\partial \tilde{\Phi}}{\partial \tilde{n}} = 0 \quad \text{(other wall boundary)}. \tag{30}$$

Galerkin procedure for equation (28) leads to the expression of weak form of

$$2\pi\iint\left(\tilde{r}\frac{\partial \tilde{\varphi}}{\partial \tilde{r}}\frac{\partial \tilde{\Phi}}{\partial \tilde{r}} + \tilde{r}\frac{\partial \tilde{\varphi}}{\partial \tilde{z}}\frac{\partial \tilde{\Phi}}{\partial \tilde{z}} - \tilde{r}\tilde{k}^2\tilde{\varphi}\,\tilde{\Phi}\right)\mathrm{d}\tilde{r}\,\mathrm{d}\tilde{z} = 2\pi\int\tilde{r}\tilde{\varphi}\frac{\partial \tilde{\Phi}}{\partial \tilde{n}}\,\mathrm{d}\Gamma, \tag{31}$$

TABLE 1

Sound pressure at several points along the central z-axis in a simple duct for various Mach numbers (the duct is terminated at one end by rigid wall $Z_T = \infty$)

M	z (m)	Analytical solution (Pa)	1D FEM	Axisymmetric FEM	Axisymmetric FEM in transformed co-ordinates	BEM
0	0·000	145·901	146·019	145·999	145·999	150·179
	0·025	395·549	395·630	395·554	395·554	403·535
	0·050	360·656	360·670	360·668	360·668	352·967
	0·075	39·140	39·105	39·104	39·104	35·022
	0·100	313·483	313·535	313·527	313·527	311·015
0·1	0·000	126·730	126·854	126·741	126·922	131·631
	0·025	385·343	385·424	385·372	385·324	394·122
	0·050	362·117	362·126	362·075	362·179	354·617
	0·075	45·693	45·656	45·595	45·717	41·744
	0·100	307·728	307·777	307·834	307·705	304·462
0·2	0·000	69·080	69·225	68·819	69·579	75·515
	0·025	356·419	356·499	356·549	356·303	366·471
	0·050	369·560	369·548	369·381	369·750	361·229
	0·075	65·968	65·918	65·676	66·176	61·550
	0·100	294·163	294·199	294·461	293·925	288·832
0·3	0·000	33·123	32·910	33·864	32·003	24·555
	0·025	311·633	311·716	312·038	311·226	325·269
	0·050	395·093	395·020	394·755	395·412	384·446
	0·075	105·029	104·941	104·370	105·597	98·676
	0·100	284·331	284·331	284·997	283·638	275·448

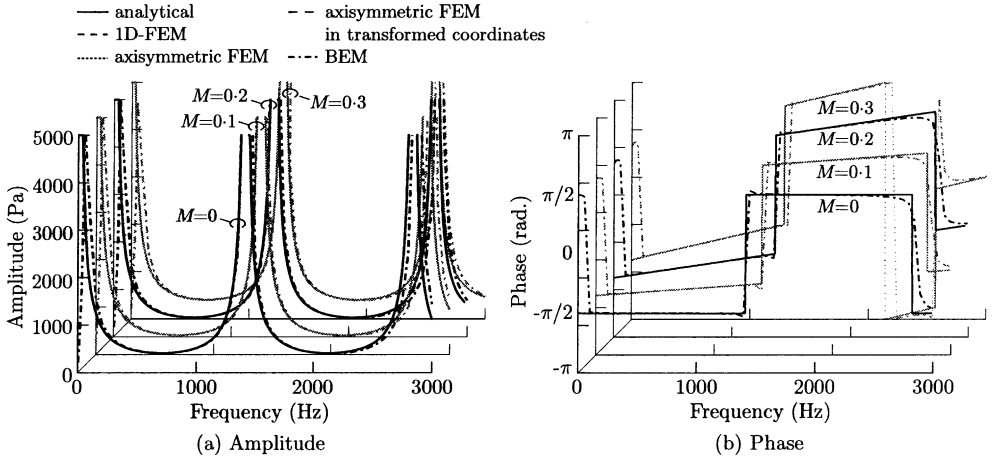

Figure 5. Frequency characteristics of the sound pressure at the termination end ($Z_T = \infty$, $z = 0{\cdot}12$ m) in the simple duct with various Mach numbers M.

where $\tilde{\varphi}$ is a weighting function. The test function, as well as the weighting function, is chosen as

$$\tilde{\Phi} = \{N\}^{\mathrm{T}}\{\tilde{\Phi}\}_e, \tag{32}$$

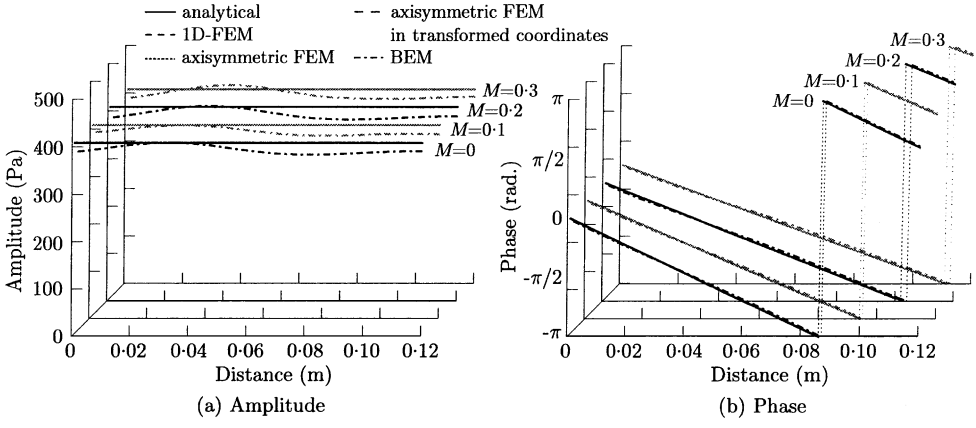

Figure 6. Sound pressure distributions along the central z-axis in the simple duct for various Mach numbers M ($f = 2$ kHz and the duct is terminated by the characteristic impedance $Z_T = \rho_0 c_0$).

TABLE 2

Sound pressure at several points along the central z-axis in a simple duct for various Mach numbers (the duct is terminated by the characteristic impedance $Z_T = \rho_0 c_0$)

M	z (m)	Analytical solution (Pa)	1D FEM	Axisymmetric FEM	Axisymmetric FEM in transformed co-ordinates	BEM
0	0·000	408·000	408·042	408·035	408·035	393·086
	0·025	408·000	408·025	407·956	407·956	406·361
	0·050	408·000	408·028	408·024	408·024	399·025
	0·075	408·000	408·045	407·972	407·972	385·829
	0·100	408·000	408·032	408·027	408·027	389·083
0·1	0·000	408·000	408·059	408·057	408·064	389·423
	0·025	408·000	408·038	407·975	407·965	406·521
	0·050	408·000	408·041	408·042	408·049	399·183
	0·075	408·000	408·062	407·994	407·985	383·477
	0·100	408·000	408·047	408·047	408·054	386·932
0·2	0·000	408·000	408·078	408·078	408·110	386·961
	0·025	408·000	408·053	407·994	407·981	407·193
	0·050	408·000	408·051	408·056	408·087	401·005
	0·075	408·000	408·078	408·016	408·004	382·672
	0·100	408·000	408·061	408·065	408·097	385·252
0·3	0·000	408·000	408·094	408·097	408·187	391·118
	0·025	408·000	408·070	408·016	408·013	412·941
	0·050	408·000	408·055	408·066	408·150	407·961
	0·075	408·000	408·092	408·035	408·035	389·497
	0·100	408·000	408·074	408·082	408·169	388·638

where $\{\tilde{\Phi}\}_e$ is the nodal velocity potential vector in the transformed co-ordinates. The discretized equation in the transformed co-ordinates is derived as

$$([\tilde{M}]_e - \tilde{k}^2[\tilde{K}]_e + \mathrm{j}\tilde{k}[\tilde{J}]_e)\{\tilde{\Phi}\}_e = U_0\sqrt{1 - M_z^2}\{\tilde{W}\}_e, \tag{33}$$

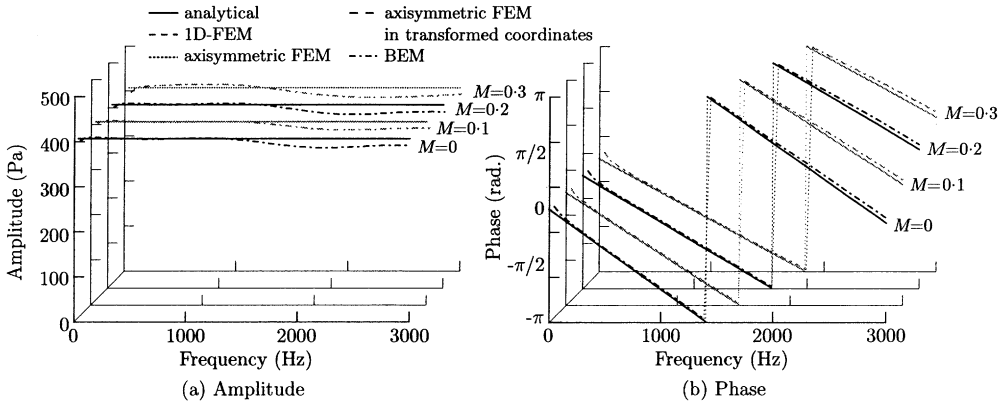

Figure 7. Frequency characteristics of the sound pressure at the termination end ($Z_T = \rho_0 c_0$, $z = 0{\cdot}12$ m) in the simple duct for various Mach numbers M.

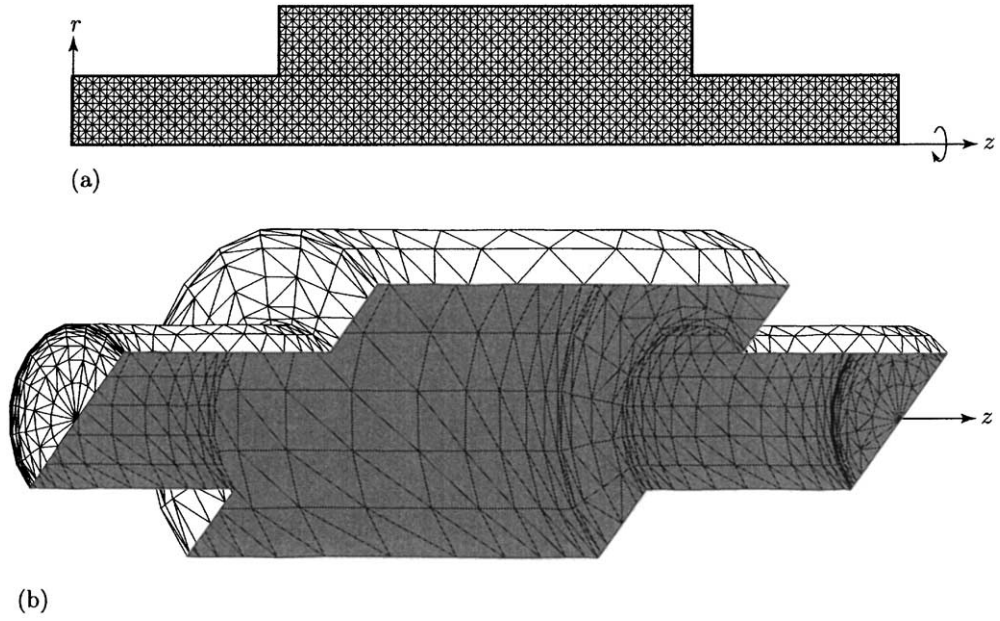

Figure 8. A muffler with expansion chamber and element division: (a) axisymmetric FEM model; (b) three-dimensional BEM model.

where $[\tilde{M}]_e$, $[\tilde{K}]_e$ and $[\tilde{J}]_e$ are inertance, elastance and damping matrix associated with the termination wall in the transformed co-ordinates and $\{\tilde{W}\}_e$ is the distribution vector in the transformed co-ordinates. The discretized equation is the same as the ordinary finite element expression. This means that the finite element program developed for the standard Helmholtz equation can be used without modification, but with the potential and the boundary conditions re-defined as given in equation (30).

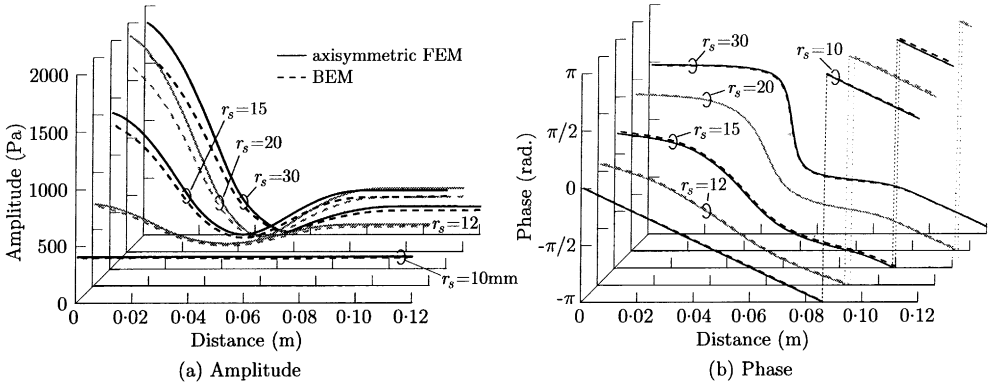

Figure 9. Sound pressure distributions along the central z-axis for various radii of the expansion chamber r_s when there is no flow ($f = 2$ kHz, $M = 0$ and the muffler is terminated by the characteristic impedance $Z_T = \rho_0 c_0$).

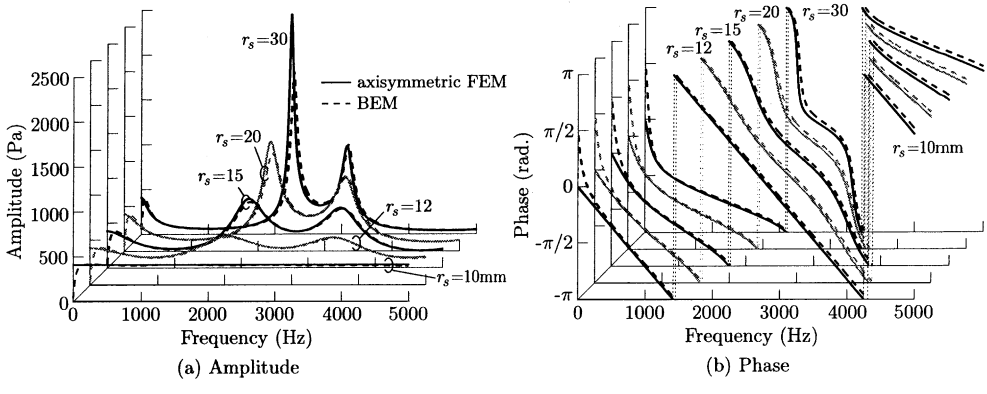

Figure 10. Frequency characteristics of the sound pressure at the termination end ($M = 0$, $Z_T = \rho_0 c_0$, $z = 0{\cdot}12$ m) for various radii of the expansion chamber r_s when there is no flow.

4.2.2. BOUNDARY ELEMENT FORMULATION

The present formulation is somewhat modified from that of Zhenlin [8]. To avoid complexity, the Helmholtz equation in the transformed co-ordinates (equation (16)) is used instead of equation (13). The boundary element integral expression corresponding to equation (16) is

$$C_i\tilde{\Phi}_i = \int_\Gamma \left(\tilde{\Phi}^* \frac{\partial \tilde{\Phi}}{\partial \tilde{n}} + \frac{\partial \tilde{\Phi}^*}{\partial \tilde{n}} \tilde{\Phi} \right) \mathrm{d}\Gamma, \tag{34}$$

where $\tilde{\Phi}^*$ is the fundamental solution

$$\tilde{\Phi}^* = \frac{1}{4\pi \tilde{R}} \mathrm{e}^{-\mathrm{j}k\tilde{R}} \tag{35}$$

which is the Green function without particular boundary condition imposed. $\tilde{R}$ is the distance from a source point to the consideration point. C_i is a coefficient related to the solid angle at point i, which becomes 1/2 if the boundary is smooth. By dividing the boundary

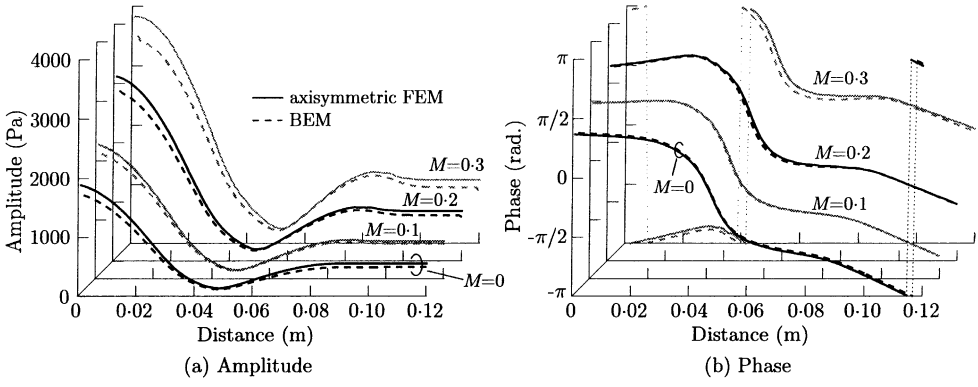

Figure 11. Sound pressure distributions along the central z-axis in the muffler for various Mach numbers M ($f = 2$ kHz, $r_s = 0{\cdot}02$ m, $Z_T = \rho_0 c_0$).

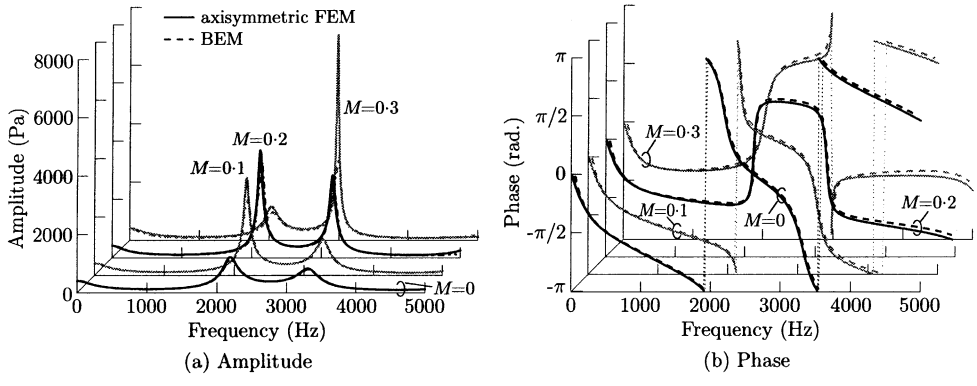

Figure 12. Frequency characteristics of the sound pressure at the termination end ($Z_T = \rho_0 c_0$, $z = 0{\cdot}12$ m) in the muffler for various Mach numbers M ($r_s = 0{\cdot}02$ m).

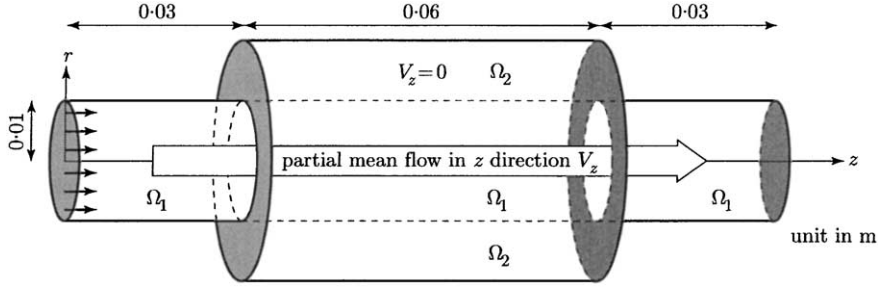

Figure 13. The muffler when mean flow is localized in the central region.

Γ into the surface boundary elements to execute an integral evaluation of equation (34), the discretized equation is obtained for the velocity potential $\tilde{\Phi}$ and the flux $\tilde{q}$ defined at the element nodes [10].

$$[\tilde{H}]\{\tilde{\Phi}\} = [\tilde{G}]\{\tilde{q}\}. \tag{36}$$

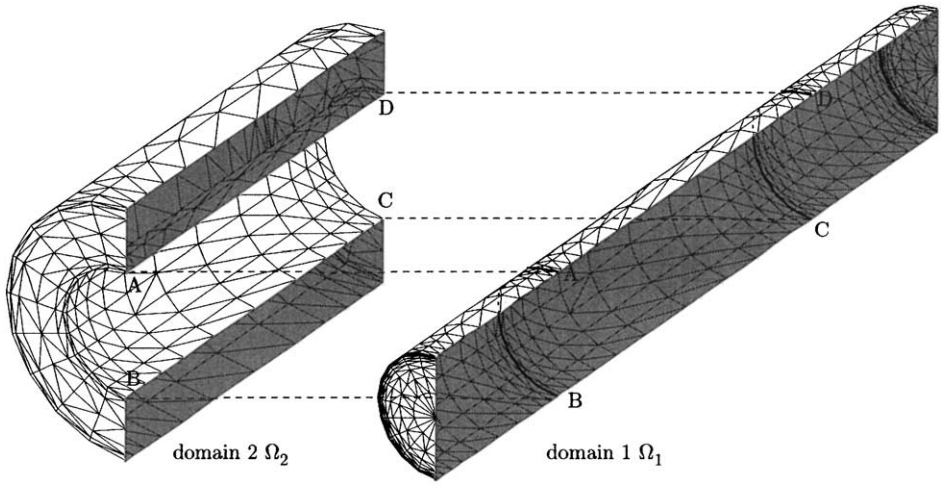

Figure 14. Partitioned boundary element model of a muffler.

With the help of equations (15) and (29), equation (36) can be transformed into the expression at original co-ordinates, so that

$$[H]\{\Phi\} = [G]\{q\}, \tag{37}$$

where

$$H_{ij} = \tilde{H}_{ij} e^{-j\tilde{k}M_z\tilde{z}_j} + j\tilde{k}M_z \frac{\partial \tilde{z}}{\partial \tilde{n}} \tilde{G}_{ij} e^{-j\tilde{k}M_z\tilde{z}_j}, \tag{38}$$

$$G_{ij} = \tilde{G}_{ij} e^{-j\tilde{k}M_z\tilde{z}_j} \frac{\partial n}{\partial \tilde{n}}, \tag{39}$$

With equation (37), no special care is required for the boundary condition at the expense that the re-evaluation of the components in the coefficient matrices must be made. The boundary element program developed for 3D acoustic field [10] cannot be used as it is, which must be modified so that the coefficient matrices are re-evaluated by equations (38) and (39).

5. NUMERICAL DEMONSTRATIONS

For the numerical demonstrations, we consider two ducts: one is a simple duct as shown in Figure 2(a) and another is a muffler with expansion-chamber as shown in Figure 2(b). The length of the ducts is $l = 0{\cdot}12$ m and the radius is 0·01 m but the expansion chamber's radius r_s is 0·01–0·03 m. The duct is driven at one end ($z = 0$) by the uniform velocity $U_0 = 1$ m/s and at another end ($z = l$), it is terminated by the sound absorber with the surface acoustic impedance Z_T. Other wall boundary is assumed to be rigid. The medium is assumed to be air ($\rho_0 = 1{\cdot}2$ kg/m^3 and $c_0 = 340$ m/s).

5.1. A SIMPLE DUCT

The finite element and the boundary element division for a simple duct are illustrated in Figure 3. The field is divided into 120 line elements for the one-dimensional FEM model.

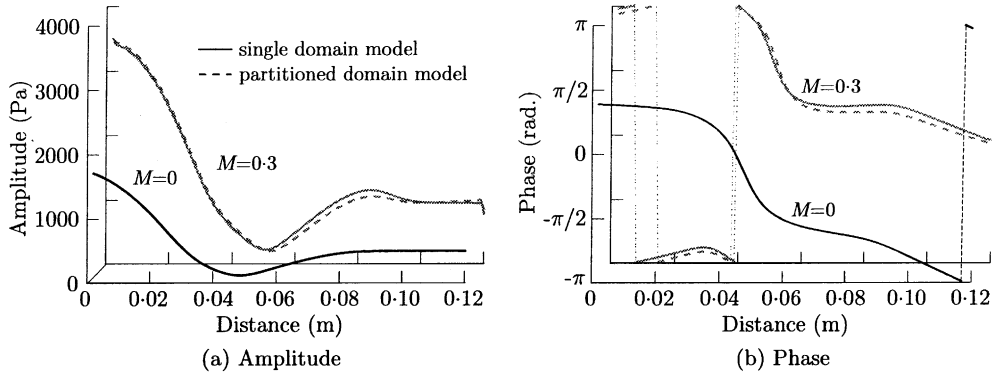

Figure 15. Comparison between the single domain model and the partitioned domain model for the sound pressure distributions along the central z-axis when the flow is uniformly presented in the muffler ($f = 2$ kHz).

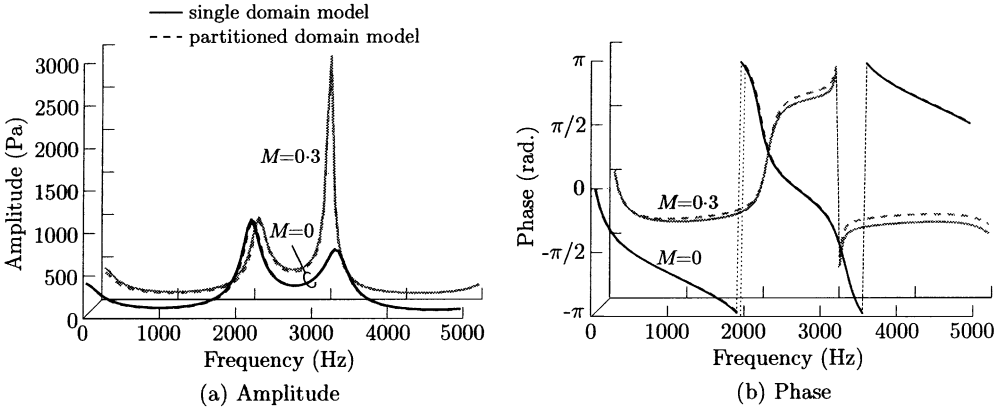

Figure 16. Comparison between the single domain model and the partitioned domain model for the frequency characteristics when the flow is uniformly presented in the muffler.

For the axisymmetric FEM model, the cross-sectional area of the field is divided into triangular ring elements, in which the division is $(z:r) = (120:10)$. For the three-dimensional BEM model, the surface of the duct is divided into 1060 triangular surface elements. The velocity potential is linearly interpolated in an element for all models. The mean flow is along the z-axis and uniform across the duct. All computations are carried out on the personal computer (VT-Alpha 533, Visual Technology-Japan, with Compaq Alpha 21164A, 533 MHz chip and 256 MB RAM) with Linux OS.

The sound pressure distributions along the central z-axis at the driving frequency of 2 kHz are shown in Figure 4, when the duct is terminated at the other end with the rigid wall ($Z_T = \infty$). The finite element solutions agree well with the analytical solution (22). As they are overlapped except the BE solutions, the sound pressures calculated by the five methods are tabulated in Table 1 for several points along the central z-axis. With the boundary element solution, the wavelength is evaluated slightly longer than the analytical solution. The transfer frequency characteristics are shown in Figure 5 for the sound pressure at the center of the termination wall when uniform mean flow is present. As the Mach number increases, the resonance peaks move lower in frequency.

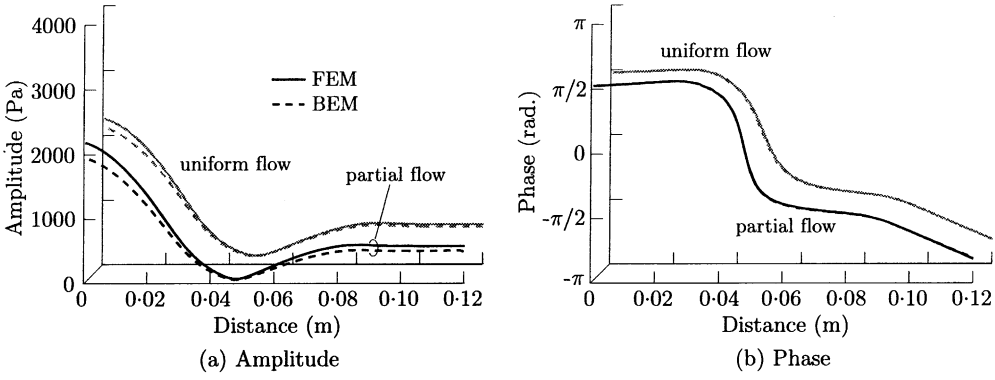

Figure 17. Comparison between the sound pressure distributions with the uniform mean flow and the partial mean flow for $M = 0{\cdot}1$ and $f = 2$ kHz.

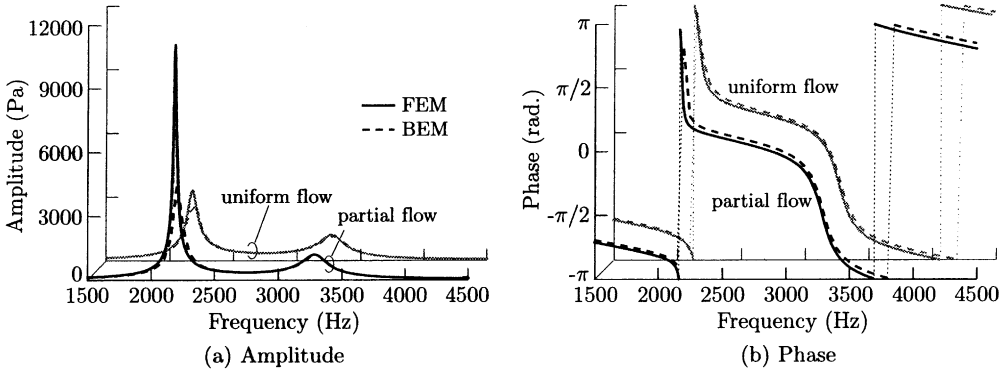

Figure 18. Comparison between the frequency characteristics with the uniform mean flow and the partial mean flow for $M = 0{\cdot}1$.

The sound pressure distributions when the duct is terminated by the characteristic impedance $Z_T = \rho_0 c_0$ are shown in Figure 6. The sound pressures calculated by the five methods are tabulated in Table 2 for several points along the central z-axis. The finite element solutions again agree well with the analytical solution within the error of 0·05%. In the boundary element solution, a slight reflection is observed. This is perhaps due to the improper discretization near the corner edges. The error is smaller in phase than the amplitude. The frequency characteristics are shown in Figure 7. The finite element solutions again show no reflection in amplitude while the boundary element solution shows an error of as much as 9·3%.

5.2. A MUFFLER WITH EXPANSION CHAMBER

The finite element division and the boundary element division of a muffler with expansion chamber are, respectively, illustrated in Figure 8. For the axisymmetric FEM model, the cross-sectional area of the field is divided into 1800 triangular ring elements. For the three-dimensional BEM model, the surface of the muffler is divided into 1300 triangular elements. The muffler is non-reflectively terminated by the characteristic impedance at the end.

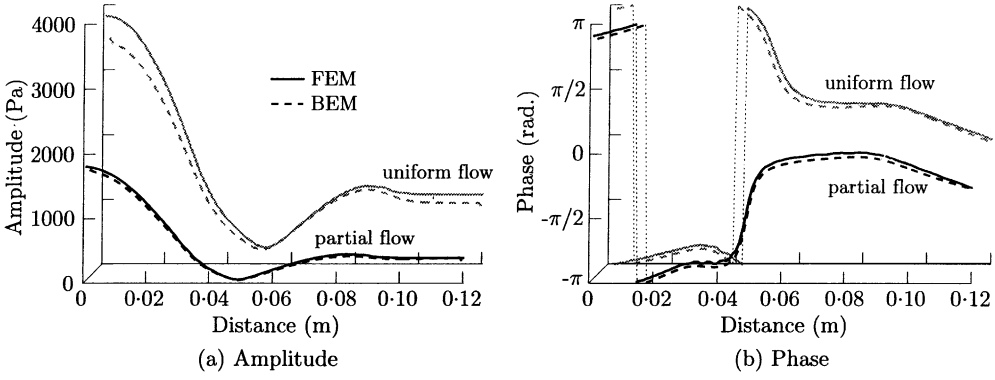

Figure 19. Comparison between the sound pressure distributions with the uniform mean flow and the partial mean flow for $M = 0{\cdot}3$ and $f = 2$ kHz.

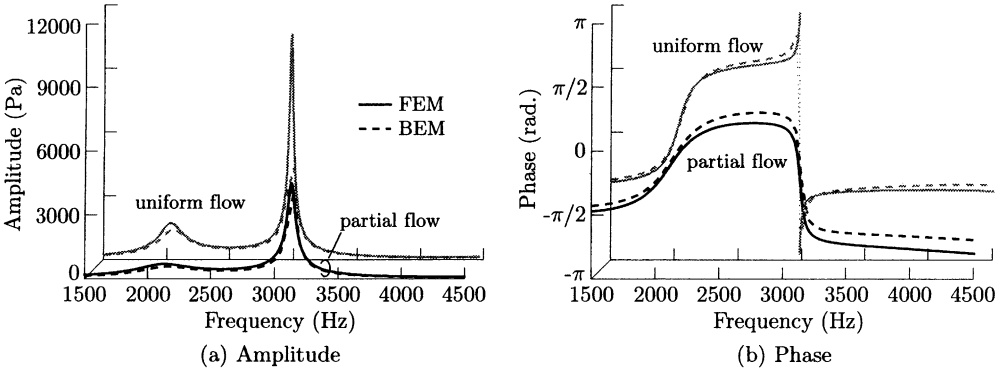

Figure 20. Comparison between the frequency characteristics with the uniform mean flow and the partial mean flow for $M = 0{\cdot}3$.

First, the case when there is no flow is considered. The sound pressure distributions along the central z-axis are shown in Figure 9 when the radius of the expansion chamber is varied. The difference in amplitude between the finite element solutions and the boundary element solutions becomes more evident for this example as the radius of the chamber increases. The element division or the element size must be responsible for this. This differences in phase are relatively small. The frequency characteristics are shown in Figure 10. There are two resonance peaks in this frequency range. The difference in peak amplitude becomes larger as the radius of the chamber increases.

Figures 11 and 12 show the sound pressure distributions and the frequency transmission characteristics of the muffler ($r_s = 0{\cdot}02$ m) when mean flow is uniformly present. There are some differences in amplitude between finite element and boundary element solutions but the differences are small in phase. The resonance peaks move lower in frequency as the Mach number increases.

5.3. CHARACTERISTICS WHEN THE PARTIAL MEAN FLOW IS PRESENT

In conventional muffler systems, however, the flow may be restricted only in the central region and may not be present in the part of the expanded chamber. Figure 13 illustrates the

model with the partial mean flow in which the flow is present only in the central duct. In order to consider the partial mean flow in the boundary element modelling, the field is divided into two domains as shown in Figure 14 in which the simple duct with the uniform mean flow (domain Ω_1) is coupled to the expansion chamber without flow (domain Ω_2). Continuity conditions are imposed over the connecting surface.

To verify the approach, the sound pressure distribution and the frequency transmission characteristic are examined, which are shown in Figures 15 and 16, in which the flow uniformly presents both in Ω_1 and Ω_2. The agreement is reasonable. Figures 17–20 show the case of the partial mean flow, when the flow only presents in domain Ω_1 for $M = 0{\cdot}1$ and $0{\cdot}3$. There are small differences between the uniform flow and the partial flow for small Mach number, while the amplitude decreases at the resonances and their peaks move lower in frequency as the Mach number increases. The effect of the presence of the partial flow on the characteristic is obvious for larger Mach numbers.

6. CONCLUDING REMARKS

The finite element and the boundary element methods are applied to the acoustic wave transmission characteristics evaluation in a medium with mean flow. For the numerical demonstrations, the one-dimensional FEM model, the axisymmetric FEM model and the three-dimensional BEM model are examined first for a straight circular duct. The solutions by the numerical approaches are compared with the analytical solution. Then, the examination is extended to the case when the mean flow is locally present in the central part of the muffler with expansion chamber. To model the spatial mean flow in the BEM model, the partitioned domain approach is developed. No shear effect between the two regions is considered. The following are the deduced conclusions:

(1) Both finite element and boundary element models give reasonable prediction for the acoustic wave transmission characteristics in a medium with mean flow, which proves the validity of the present modellings.
(2) The resonance peaks move lower in frequency as the Mach number increases.
(3) The effect of the presence of the partial flow is more pronounced as the Mach number increases.

REFERENCES

1. C. J. YOUNG and M. J. CROCKER 1975 *Journal of Acoustical Society of America* **57**, 144–148. Prediction of transmission loss in mufflers by the finite element method.
2. Y. KAGAWA and T. OMOTE 1976 *Journal of Acoustical Society of America* **60**, 1003–1013. Finite element simulation of acoustic filters of arbitrary profile with circular cross-section.
3. Y. KAGAWA, T. YAMABUCHI and A. MORI 1977 *Journal of Sound and Vibration* **53**, 357–374. Finite element simulation of an axisymmetric acoustic transmission system with a sound absorbing wall.
4. Y. KAGAWA, T. YAMABUCHI and S. MINAMIBAYASHI 1977 *Transactions of the Institute of Electronics and Communication Engineers* **J60-A**, 1138–1145. Finite element simulation of acoustic ducts (in Japanese).
5. Y. KAGAWA, T. YAMABUCHI, T. YOSHIKAWA, S. OOIE, N. KYOUNO and T. SHINDOU 1979 *Journal of Sound and Vibration* **69**, 207–228. Finite element approach to acoustic transmission-radiation systems and application to horn and silencer design.
6. M. L. MUNJAL 1987 *Acoustics of Ducts and Mufflers*. New York: Wiley-Interscience.
7. CHATTAJEE 1990 *Ph.D. Dissertation. Indian Institute of Science, Bangarol.*
8. J. ZHENLIN, M. QIANG and Z. ZHINHUA 1994 *Journal of Sound and Vibration* **173**, 57–71. Application of the boundary element method to predicting acoustic performance of expansion chamber mufflers with mean flow.

9. Y. KAGAWA, T. TSUCHIYA, T. HARA and T. TSUJI 2001 *Journal of Sound and Vibration* **246**, 419–439. Discrete Huygens' modelling simulation of sound wave propagation in velocity varying environments.
10. Y. KAGAWA, R. SHIMOYAMA, T. YAMABUCHI, T. MURAI and K. TAKARADA 1992 *Journal of Sound and Vibration* **157**, 385–403. Boundary element models of the vocal tract and radiation field and their response characteristics.